The Behavior of Slab-Column Joints of Reactive Powder Concrete under Cyclic Load

Bambang Budiono[1,*], Awal Surono[1], Ivindra Pane[1] & Ruddy Kurniawan[2]

[1]Faculty of Civil and Environmental Engineering,
Institute of Technology Bandung, Jalan Ganesha 10 Bandung, Indonesia
[2]Department of Civil Engineering, Andalas University
Kampus Teknik Unand Limau Manis, Pauh, Padang 25163, Indonesia
*E-mail: b.budiono1995@gmail.com

Abstract. Experimental work on four specimens of reinforced concrete slab-column connection sub-assemblages using reactive powder concrete (RPC) was conducted. The specimens were subjected to a combination of gravity and cyclic loading. The gravity loading was represented by a number of concrete cubes hung on the slab bottom surface and the cyclic lateral loading was applied on the upper end of the columns. The specimens consisted of two variables, i.e tensile flexural reinforcement ratio (0.65% and 1.8%) and slab span (2.0 m and 3.0 m). Shear reinforcement was not used in the slab. The displacement history consisted of three repeated cycles, starting from 0.07 to 5.00 percent drift ratio, covering the elastic and the inelastic response of the specimens. The RPC mixture proportion for the specimen's material was developed using local materials and normal concrete technology methods. The average RPC compression tests results were 136.0 MPa at 28 days and 141.0 MPa at the time of the first specimen, tested at 56 days. The tests results showed that up to 5.0 percent drift all specimens had stable hysteresis loops without any significant degradation of strength and stiffness. The specimen with a larger tensile flexural reinforcement ratio developed more strength, stiffness and energy dissipation.

Keywords: *gravity loading; hysteretic behavior; lateral cyclic loading; reactive powder concrete; slab-column joint sub-assemblage.*

1 Introduction

Flat slab reinforced concrete structures are recognized as more economical compared to the normal structures which use beams and slabs in view of reducing the height of inter-story floors. However, in the case of open-frame structures under a combination of gravity and cyclic loading during seismic excitation, a large shear force will develop on the slab at the column face leading to progressive punching shear failure under a brittle mechanism. Therefore, for seismic-prone areas, ductile flat slab structures should be combined with shear walls forming a dual structural system, where shear walls should be able to resist a maximum of 75.0 percent of the seismic load.

Received March 7th, 2016, Revised August 9th, 2016, Accepted for publication August 31st, 2016.
 ISSN: 2337-5779, DOI: 10.5614/j.eng.technol.sci.2016.48.4.4

Several alternative solutions are available to enhance the slab's shear strength. One solution is to increase the thickness of the slab or to develop a slab capital at the column perimeter (drop panel). Drop panels improve the strength and stiffness of the flat slab, however, the ductility and the energy dissipation are relatively low [1]. Another option is to use shear reinforcement or shear studs surrounding the column. Gunadi, *et al*. [2] have successfully developed a new design of shear studs for seismic resistant flat slabs showing good hysteretic behavior under cyclic loading. However, the detailing of the shear studs is uneconomical.

Another alternative to enhance the slab's shear strength is to improve the concrete strength and/or a combination of the previous options. Previous investigations [3] have shown that the use of high-strength concrete slab improves shear strength and ultimate displacement, leading to more ductile flat-slab structures.

To improve the seismic resistance performance of flat-slab structures, steel fibers are added in a high-strength concrete mix. Steel fibers have been proven to enhance the shear strength, stiffness, ductility and energy dissipation of the structure as well as decreasing crack width [4].

In this investigation, ultra-high strength concrete was developed using reactive powder concrete (RPC) for experimental work on slab-column joint sub-assemblages under cyclic loading [5]. The concrete mix of RPC comprised of local materials and simple concrete mix technology was used with neither steam curing nor pre-setting pressure. The parameters of the experimental work were tensile reinforcing bar length and span length. Several researches using normal concrete [6-7] have shown that reinforcing the tensile bar ratio influences the shear capacity of the slab-column joint significantly. The span-length parameters were used to observe the hysteretic behavior on the structure either under flexural or shear dominated action.

2 Experimental Set-up

2.1 Materials

For the RPC mix, portland cement ASTM C150 [8] Type II consisting of C_3A at approximately 6.0 percent was used. Aggregate materials were quartz sand and quartz powder with particle sizes of 600.0 and 50.0 micrometers, respectively. To improve the paste mechanical properties, silica fume was added in the RPC mix to comply with the ASTM C 1240 [9] standard. To improve the workability of the mix, poly-carboxylate-based super-plasticizer was used in accordance with type F of the ASTM C 494-92 [10] standard. Some polypropylene fibers

with a length of 12.0 mm and a diameter of 0.2 mm were added to the mix to avoid initial cracks due to shrinkage of the RPC mix. All RPC materials were mixed using local materials. The ratios of each material to the total weight of the mix are presented in Table 1.

Table 1 Ratio of material to total weight of RPC mix.

Material	Weight ratio (%)
Cement	39.00
Silica fume	5.00
Quartz sand	43.00
Quartz powder	3.00
Water	9.00
Super-plasticizer	0.98
Polypropylene fiber	0.02
Total	**100.00**

The RPC was mixed at once in the same batch in order to obtain the same compressive and tensile strength properties for the mix as well as the specimens of the slab-column joints. Normal and simple concrete technology was used for curing. The curing of the concrete specimens was conducted using a water puddle on the concrete surface. There was no pre-setting pressure or steam curing on the specimens. The treatment used for the concrete cylinders was the same as for the specimens. The average cylinder compression test results for diameters of 100.0 mm and 200.0 mm were 136.0 MPa after 28 days and 141.0 MPa on the day of the test (56 days).

2.2 Test Specimens

Tests were conducted on 4 specimens of slab-column joint sub-assemblages at half scale. The parameters were the tensile reinforcing bar ratio (ρ) and the span length of the slab. The dimensions and the details of the reinforcing bars were as shown in Figure 1 and the material properties of the slab of specimens were as shown in Table 2. For each specimen, both ends of the slab were supported by rollers while the bottom of the column rested on a pin.

The ratio between the top and bottom of the reinforcing bar was equal to 0.7. No shear reinforcement was used. Therefore the shear force due to gravity and cyclic load was resisted by the concrete and the dowel action of the longitudinal reinforcement. The specimens were provided with reinforcing bars of 8.0 and 13.0 mm diameter, as shown in Figures 2 and 3.

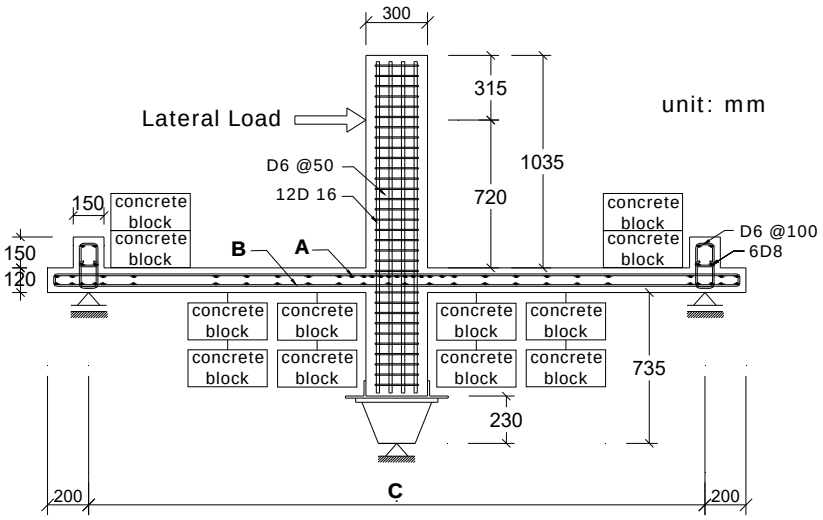

Notation	Specimen			
	L3R065	L3R18	L2R065	L2R18
A (top rebar)	D8 @100	D13 @100	D8 @100	D13 @100
B (bottom rebar)	D8 @150	D13 @150	D8 @150	D13 @150
C (slab length)	3000 mm	3000 mm	2000 mm	2000 mm

Figure 1 Dimensions and reinforcing bar of the specimens.

Table 2 Specimen properties.

Specimen	Slab dimensions (mm), Length x width x thickness	ρ (%)	f_c' (MPa)	f_y (MPa)	ρf_y (MPa)
L3R065	3000 × 1500 × 120	0.65	141	404	2.6
L3R18	3000 × 1500 × 120	1.8	141	456	7.2
L2R065	2000 × 1000 × 120	0.65	141	404	2.6
L2R18	2000 × 1000 × 120	1.8	141	456	7.2

The parameters for the span length consisted of a long slab span of 3.0 x 1.5 x 0.12 m and a short slab span of 2.0 x 1.0 x 0.12 m representing flexural and shear dominated action, respectively. The width of the slab was considered as the effective column width of the slab.

The column dimensions for all specimens were 300.0 x 300.0 mm (see Fig. 1). The reinforcing bar for the column was 12 bar @ 16 mm diameter with a yield strength of 542.0 MPa and the shear reinforcement bar was 6.0 mm diameter @ 50 mm spacing with a yield strength of 355 MPa.

The column was designed using the strong column-weak beam concept to comply with the ACI 318 [11] standard. For lifting purposes, a beam was cast monolithically at each end of the slab (see Figure 1).

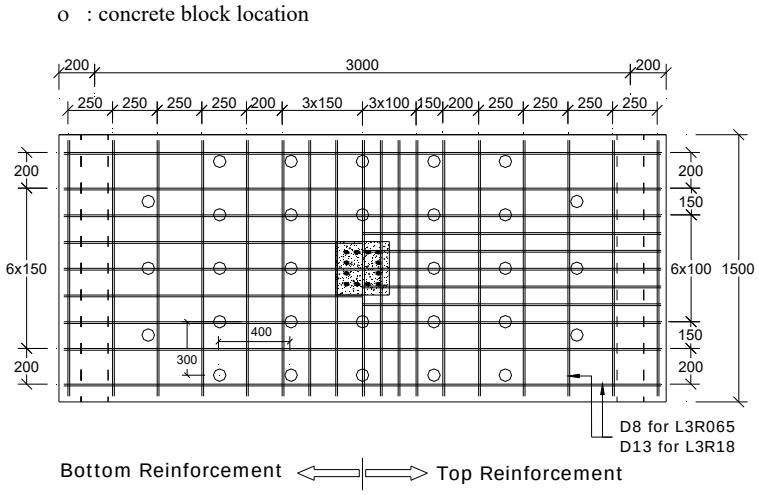

Figure 2 Reinforcement of long span slab.

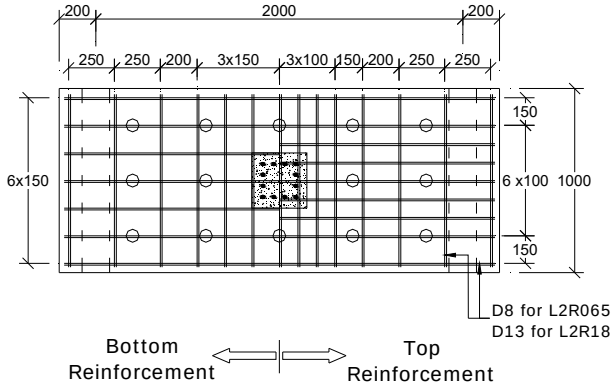

Figure 3 Reinforcement of short span slab.

2.3 Test Set-up and Instrumentation

During the test, the slab was positioned horizontally and the column was set up vertically. Lateral cyclic loading was provided using an actuator positioned horizontally at the end of the column. The bottom of the column rested on a pin

while it had a free end at the upper part, as shown in Figure 1. The slab was simply supported using a roller and a pin located at the ends of the slab.

Several strain gauges were mounted at the top and bottom reinforcing bars within a distance of 0.5 d from the column face, where *d* is the effective height of the slab. At the top of the column, a displacement transducer (LVDT) was mounted coincident with the lateral force center line of the actuator to measure the lateral cyclic displacement of the column. Lateral LVDT's were also set up at both supports of the slab to assure that the supports were laterally practically motionless. The roller and the pin of the slab's supports were held down on the steel frames, which were designed to have negligible vertical movement.

2.4 Loading Set-up

The loading of the specimen consisted of a combination of gravity (as permanent load) and cyclic lateral loadings. Gravity load was 8.45 kN/m^2 using suspended concrete blocks of 200 x 300 x 300 mm^3 equally distributed at the bottom of the slab as shown in Figure 4. The positions of the concrete blocks are shown in Figure 2. The individual weight of each concrete block was in the range of 400.0 to 440.0 kN. To simulate the gravity load, gravity loading was applied prior to the seismic loading. All concrete blocks were then hung on slabs as balance cantilevers before the roller and pin were set up. Consequently, the slabs underwent initial vertical deflection due to the gravity loading only prior to cyclic loading.

Figure 4 Loading set-up with specimens.

Lateral cyclic loading was applied to the specimens incrementally, complying with the ACI 374 [12] standard using incremental displacement control measured at the upper end of the column. In each stage of displacement control, three repeated cycles were used to observe the strength and the stiffness degradation. The lateral cyclic load was terminated until either the specimen

collapsed or the maximum capacity of the actuator was reached at a drift of around 5.0 percent. The cyclic loading sequence is shown in Figure 5.

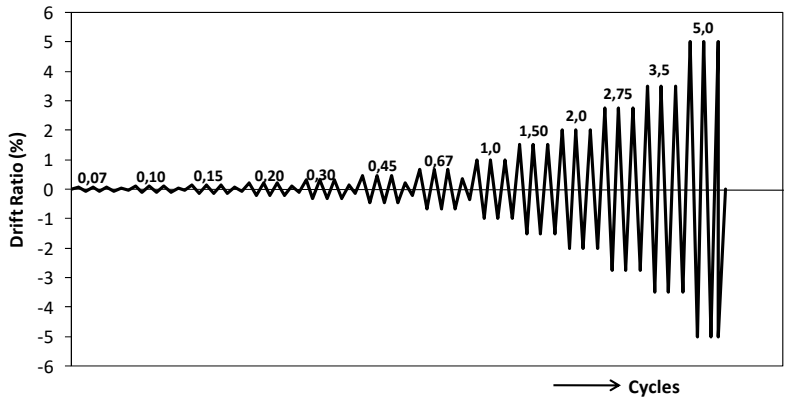

Figure 5 Cyclic loading sequence.

3 Test Results and Discussions

3.1 Crack Patterns

When the gravity loading was fully applied prior to the lateral loading, it was found that no cracks had developed in any of the specimens. Cracks in all specimens occurred when the displacement drift ratio was 0.15 percent. At this stage, the cracks were distributed from the column face to the near end of the slabs. The crack patterns at this stage cut the slab vertically, showing that flexural cracks dominated both for long and short spans. For the following drift, more cracks developed on the column face with a pattern of flexural shear cracks.

At a 5.0 percent drift ratio, the test was terminated because the maximum capacity of the actuator was reached. Figures 6 and 7 show the crack patterns at the final drift of 5.0 percent. It can be seen that that the cracks at a larger reinforcement ratio (ρ = 1.8% for L3R18 and L2R18) were spread more widely compared to a smaller rebar ratio (ρ = 0.65% for L3R065 and L2R065). The spread of the crack patterns was relatively similar for the same reinforcement ratio for both the long and the short span (L3R18 compared to L2R18 and L3R065 compared to L2R065). The ratio of the tensile reinforcing bar influenced the characteristics of the crack patterns rather than the difference in slab span.

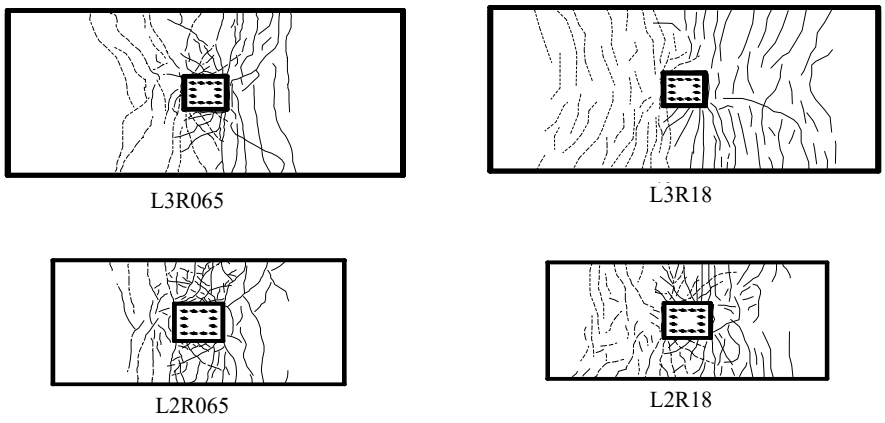

Figure 6 Crack patterns at 5.0 percent drift.

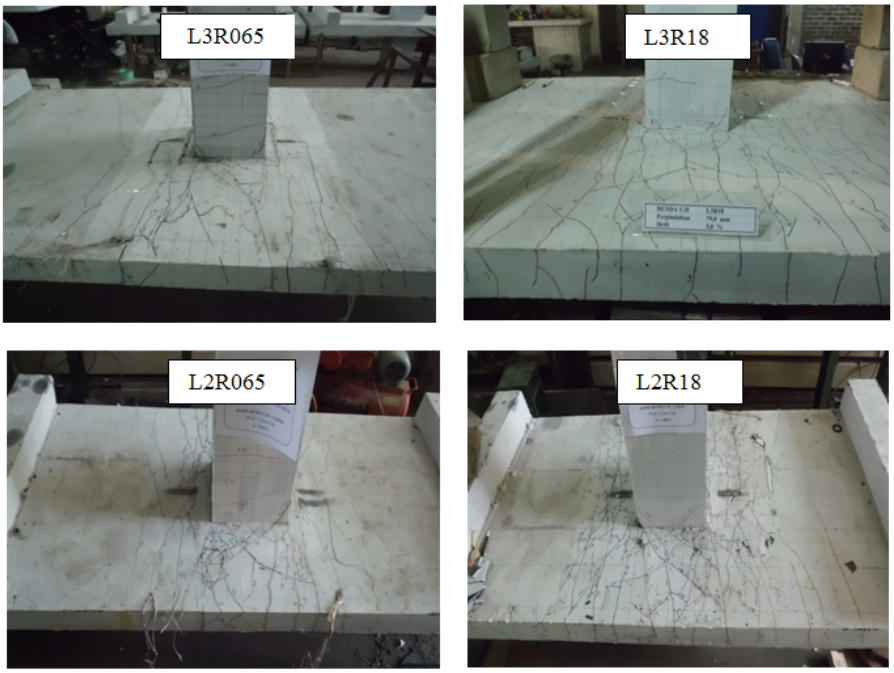

Figure 7 Photographs of crack patterns at 5.0 percent drift.

3.2 Load-drift Relationship

Figure 8 shows the hysteretic behavior results for all specimens. The cyclic displacement, presented in terms of drift ratio, is defined as the ratio between the top lateral displacement of the column and the total column's height.

Figure 8 shows that the hysteretic loops are stable until a 5-percent drift ratio without any significant degradation for either stiffness or strength. There was no shear and/or punching shear failure at the 5-percent drift ratio. As no shear reinforcement was present, the shear force had to be carried by the high shear strength of the RPC together with the dowel action provided by the flexural reinforcement. The combination of these actions is capable of preventing shear and/or punching shear failures until a drift ratio of 5 percent, which is 3.5 percent higher than required by ACI 374 [12].

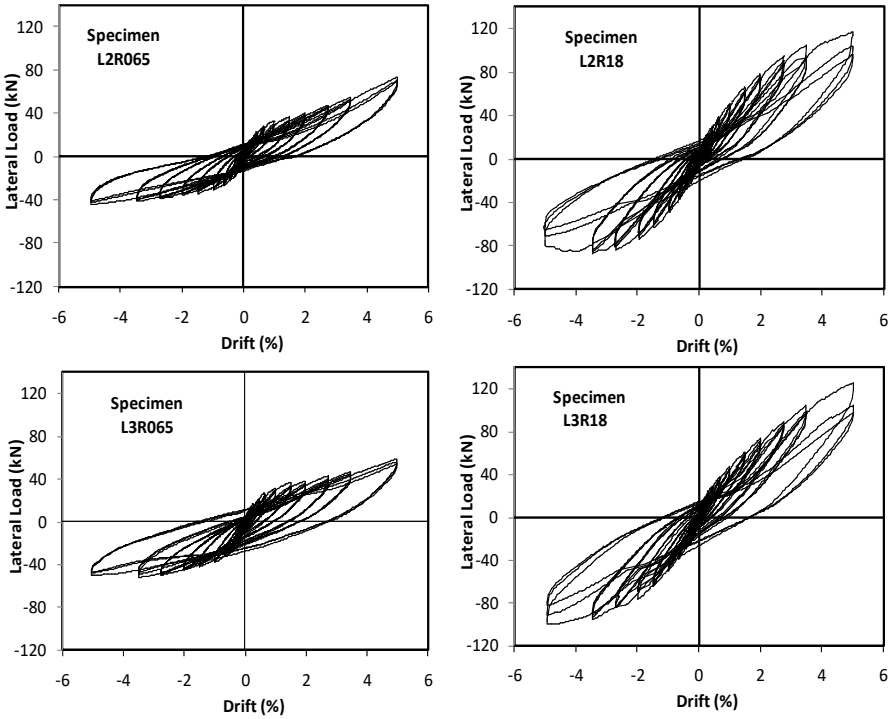

Figure 8 Hysteretic behaviors of all specimens.

The maximum lateral force of each specimen is presented in Table 3. After cracking of the RPC, as mentioned earlier, the shear force was resisted by the RPC with dowel action only and without aggregate interlock. The contribution

of aggregate interlock was insignificant because the maximum diameter of the RPC aggregate was around 0.6 mm.

Table 3 Peaks of hysteretic load.

Specimen	Peak load (+) (kN)	Drift at peak load (%)	Peak load (–) (kN)	Drift at peak load (%)	Ratio between peak loads (–) / (+)
(1)	(2)	(3)	(4)	(5)	(6) = –(4) / (2)
L3R065	58.6	5.0	–52.2	–3.5	0.89
L3R18	124.9	5.0	–99.9	–5.0	0.80
L2R065	73.3	5.0	–43.9	–5.0	0.60
L2R18	116.8	5.0	–86.7	–3.5	0.74

3.3 Strain of Flexural Reinforcement

The strain gauge readings on the left hand side (LHS) of the slab showed that the flexural reinforcement next to the column face commenced yielding at drifts of 0.45, 1.50, 0.67 and 1.5 percent each for the specimens L3R065, L3R18, L2R065 and L2R18, respectively. The relationship between the drift and the strain gauge readings at the top flexural reinforcing bar next to the column face is shown in Figure 9.

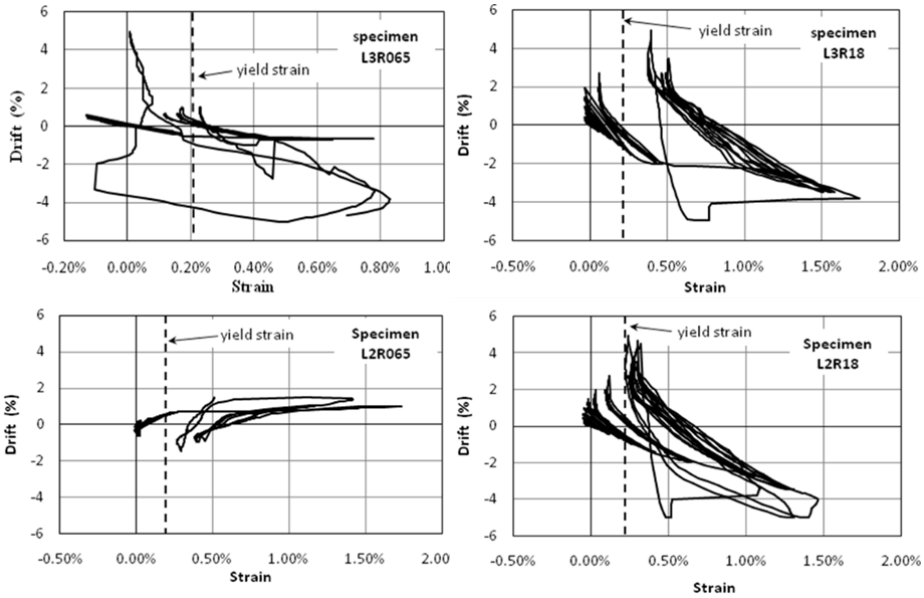

Figure 9 Drift vs. strain of top rebar at LHS of the slab next to the column face.

When the actuator reached its maximum capacity of 5.0 percent, the test was terminated; therefore it was difficult to determine the ultimate capacity and the ductility of the specimens. The first yield of the reinforcement with a smaller flexural reinforcement ratio occurred at an earlier stage. The reason for this phenomenon is the very high strength of RPC, which in turn develops a shorter neutral axis height leading to a larger curvature. Therefore, the smaller flexural reinforcement ratio, the larger the flexural strain at the first yielding at a small drift ratio. Meanwhile, the influence of the span length is insignificant to the strain at the first yielding.

3.4 Energy Dissipation

The input of the hysteretic energy, absorbed by the specimen, is the energy dissipation, which was calculated as the cumulative areas of the curves of the relationship between load and deformation of each cyclic loading cycle. The energy dissipation of the specimens L3R065, L3R18, L2R065 and L2R18 at drift ratio of 5% was 9.76, 10.29, 8.25 and 10.42 kNm, respectively. The reinforcement ratio has a significant influence on energy dissipation. The energy dissipation increases as the reinforcement ratio increases. To satisfy that the structures have sufficient damping during seismic excitation, ACI 374 [12] requires the energy dissipation ratio (β) of the third cycle, at a 3.5% drift ratio, to be at least 1/8. The definition of β is as shown in Figure 10. Figure 10 shows the ratio between the actual energy dissipation of the structure represented by the area of the hysteretic loop and the area of the ideal energy dissipation represented by the area of the pararellogram A-B-C-D-F-G-A. Table 4 shows the β ratio of all specimens at the third cycle at a 3.5% drift ratio. The results reveal that all specimens had sufficient damping to withstand a major earthquake. Under a lower ratio of tensile reinforcement the specimens had a larger damping ratio.

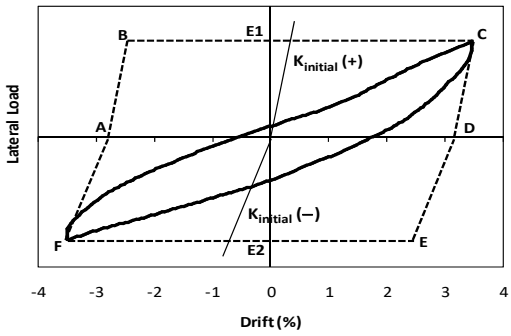

Figure 10 Definitions for relative energy dissipation (β).

Table 4 β Ratio under 3.5% drift ratio at the 3rd cycle.

Specimen	Initial Stiffness		Area of Paralelogram	Area of hysteresis loop	β
	$K_{initial}$ (+)	$K_{initial}$ (-)	A_p	A_h	A_h/A_p
	kN/mm	kN/mm	kN/mm	kN/mm	
L3R065	8.78	9.09	9130.95	2293.62	1/3.98
L3R18	8.58	8.45	16505.57	2194.18	1/7.52
L2R065	5.45	7.98	8687.99	1921.04	1/4.52
L2R18	12.58	11.69	16940.30	2602.86	1/6.51

4 Conclusion and Future Research

Testing of four specimens of slab-column joints made of RPC was conducted experimentally under a combination of gravity and cyclic loading. The following conclusions can be drawn from the test results.

The ultra-compression strength of RPC is capable of improving the shear strength of the slab. All specimens withstood a 5% inelastic drift ratio under stable conditions without any punching shear failures. When the ratio of the top reinforcing bar was increased, the energy dissipation increased but the development of yielding of the top reinforcement was delayed.

Longer slabs resulted in larger energy dissipation but the first yielding commenced earlier at the top reinforcement. The influence of the ratio of the top reinforcement was more significant compared to the span length in terms of the energy dissipation ratio.

All specimens satisfied the energy dissipation ratio requirements from the ACI 374 standard [12]. Therefore, the damping of all specimens was sufficient to withstand a credible seismic load.

As for future research, it is important to investigate some additional parameters, such as the influence of slab thickness. Also important is the development of a non-linear finite element model to find the stress distribution of the specimens under cyclic loading. Enlarging the slab thickness will improve the stiffness of the slab significantly. It is important to find the optimum ratio between thickness and clear span under cyclic loading. The use of a non-linear finite element model enables prediction of the stress distribution of the specimens, particularly the hysteretic stress behavior of the plastic hinges.

Acknowledgements

The authors would like to acknowledge and convey their sincere gratitude to the Directorate General of Higher Education for the Higher Education Decentralization Priority Research Grant of ITB Year 2012 under contract no. 003.40/TL – J/DIPA/SPK/2012.

References

[1] Megally, S. & Ghalli, A., *Seismic Behavior of Slab-Column Connections,* Canadian Journal of Civil Engineering, **27**, pp. 84-100, 2000.

[2] Gunadi, R., Budiono, B., Imran, I. & Sofwan, A., *The Behavior of Slab-Column Connections with Modified Shear Reinforcement under Cyclic Load*, Journal of Engineering and Technological Sciences, **46**(1), pp. 17-36, 2014.

[3] Emam, M., Marzouk, H. & Hilal, M.S., *Seismic Response of Slab-Column Cnnections Constructed with High Strength Concrete*, ACI Structural Journal, **94**(2), pp. 197-205, 1997.

[4] Cheng, M.Y. & Montesinos, G.J.P., *Evaluation of Steel Fiber Reinforcement for Punching Shear Resistance in Slab-Column Connections—Part II: Lateral Displacement Reversals*, ACI Structural Journal, **107**(1), pp. 110-118, 2010.

[5] Kurniawan, R., *The Behavior of Slab-Column Joint of Reactive Powder Concrete Under Combination of Gravity and Lateral Cyclic Loadings (in Indonesian)*, PhD Dissertation, Department of Civil Engineering, Institute of Technology Bandung, Bandung, 2015.

[6] Tian, Y., Jirsa, J.O. & Bayrak, O., *Strength Evaluation of Interior Slab Column Connections*, ACI Structural Journal, **105**(6), pp. 692-700, 2008.

[7] Guandalini, S., Burdet, O.L. & Muttoni, A., *Punching Tests of Slabs with Low Reinforcement Ratios*, ACI Structural Journal, **106**(1), pp. 87-95, 2009.

[8] ASTM C150-04a, *Standard Specification for Portland Cement*, ASTM International, United States, 2004

[9] ASTM C1240-00, *Standard Specification for Silica Fume used in Cementitious Mixtures*, ASTM International, United States, 2000

[10] ASTM C494-92, *Standard Specification for Chemical Admixtures for Concrete*, ASTM International, United States, 1992

[11] ACI Commite 318, *Building Code Requirements for Structural Concrete and Commentary (ACI 318–11)*, American Concrete Institute, 2011

[12] ACI Committee 374, *Acceptance Criteria for Moment Frames Based on Structural Testing and Commentary (ACI 374.1–05)*, American Concrete Institute, 2005.